Growth-speed-correlated localization of exocyst and polarisome components in growth zones of *Ashbya gossypii* hyphal tips

Michael Köhli[1], Virginie Galati[1], Kamila Boudier[1], Robert W. Roberson[2] and Peter Philippsen[1,*]

[1]Biozentrum, University of Basel, Klingelbergstrasse 50/70, 4056 Basel, Switzerland
[2]School of Life Sciences, Arizona State University, Tempe, AZ 85287, USA
*Author for correspondence (e-mail: peter.philippsen@unibas.ch)

Accepted 27 August 2008
Journal of Cell Science 121, 3878-3889 Published by The Company of Biologists 2008
doi:10.1242/jcs.033852

Summary

We use the fungus *Ashbya gossypii* to investigate how its polar growth machinery is organized to achieve sustained hyphal growth. In slowly elongating hyphae exocyst, cell polarity and polarisome proteins permanently localize as cortical cap at hyphal tips, thus defining the zone of secretory vesicle fusion. In tenfold faster growing hyphae, this zone is only slightly enlarged demonstrating a capacity of hyphal growth zones to increase rates of vesicle processing to reach higher speeds. Concomitant with this increase, vesicles accumulate as spheroid associated with the tip cortex, indicating that a Spitzenkörper forms in fast hyphae. We also found spheroid-like accumulations for the exocyst components *Ag*Sec3, *Ag*Sec5, *Ag*Exo70 and the polarisome components *Ag*Spa2, *Ag*Bni1 and *Ag*Pea2 (but not *Ag*Bud6 or cell polarity factors such as *Ag*Cdc42 or *Ag*Bem1). The localization of *Ag*Spa2, *Ag*Pea2 and *Ag*Bni1 depend on each other but only marginally on *Ag*Bud6, as concluded from a set of deletions. Our data define three conditions to achieve fast growth at hyphal tips: permanent presence of the polarity machinery in a confined cortical area, organized accumulation of vesicles and a subset of polarity components close to this area, and spatial separation of the zones of exocytosis (tip front) and endocytosis (tip rim).

Supplementary material available online at
http://jcs.biologists.org/cgi/content/full/121/23/3878/DC1

Key words: Filamentous fungus, Spitzenkörper, Polar growth, Exocytosis, Cdc42, Bni1, Yeast

Introduction

Filamentous fungi comprise a large group of very diverse species. Some are beneficial, others cause devastating plant diseases or are becoming increasingly notorious as human pathogens (Harris et al., 2005). They grow as multinucleated tubular cells called hyphae by polar surface expansion at their tips (Bartnicki-Garcia and Lippman, 1969). Expansion of the plasma membrane and the fungal cell wall requires continuous incorporation of lipids and cell wall components, which are synthesized throughout the hyphae before being transported to the tip by secretory vesicles. In some species, hyphal surface expansion rates can amount to 100 μm^2/minute, much higher than the well-studied growth of yeast buds, which expand at around 1 μm^2/minute (Collinge and Trinci, 1974; Karpova et al., 2000; Park and Bi, 2007).

One hallmark of fungal polar growth is the persistent tip localization of polarity markers that, in budding yeast, only transiently localize to tips of daughter cells. Examples are the formins SepA and Bni1 (Ozaki-Kuroda et al., 2001; Schmitz et al., 2006; Sharpless and Harris, 2002), the p21 activated protein kinase Cla4 (Ayad-Durieux et al., 2000; Holly and Blumer, 1999) and the polarisome component Spa2 (Crampin et al., 2005; Knechtle et al., 2003; Snyder, 1989; Virag and Harris, 2006). The mechanisms leading to the differences between stable and transient localization of polarity factors are not known. However, it has been noted that cortical actin patches do not localize to the entire hyphal tip, leaving at its front a confined space for polar growth components (Knechtle et al., 2003; Taheri-Talesh et al., 2008).

Another hallmark of hyphal growth is the tip-located Spitzenkörper (German for 'tip body'), a complex multicomponent structure dominated by vesicles (reviewed by Harris et al., 2005; Steinberg, 2007). Computer simulations suggest that it serves as vesicle supply centre at hyphal tips (Bartnicki-Garcia et al., 1989; Gierz and Bartnicki-Garcia, 2001). Proteins that are commonly associated with secretory vesicles are found in the Spitzenkörper like a v-SNARE in *Aspergillus nidulans* (Taheri-Talesh et al., 2008) or cell wall synthesizing enzymes in *Neurospora crassa* (Riquelme et al., 2007). In addition, the GTP-binding protein Sec4, a regulator of vesicle transport and fusion, takes a Spitzenkörper-like shape in hyphal tips of *Ashbya gossypii* (Schmitz et al., 2006). Furthermore, filamentous actin (f-actin) is required for the Spitzenkörper as the Spitzenkörper is sensitive to disruption of the actin cytoskeleton (Crampin et al., 2005; Taheri-Talesh et al., 2008) and as formins, which catalyze actin cable polymerization, are found in the Spitzenkörper of different species (Crampin et al., 2005; Harris et al., 2005).

We study hyphal growth of the cotton pathogen *A. gossypii* (Ashby and Nowell, 1926). Its genome shows 92% gene order conservation with the *Saccharomyces cerevisiae* genome (Dietrich et al., 2004). Analogous to *S. cerevisiae*, secretory vesicles are believed to arrive at hyphal tips via myosin-dependent transport along actin cables. These vesicles are tethered to the plasma membrane by the exocyst and fuse. The exocyst is a conserved complex that consists of eight components in budding yeast: *Sc*Exo70, *Sc*Exo84, *Sc*Sec3, *Sc*Sec5, *Sc*Sec6, *Sc*Sec8, *Sc*Sec10 and *Sc*Sec15. The exocyst was shown to be essential for fusion of

secretory vesicles and is found at sites of exocytosis in *S. cerevisiae* daughter cells and the forming septum (Finger et al., 1998; Guo et al., 1999; TerBush et al., 1996). It interacts with factors that control polar growth such as *Sc*Cdc42, *Sc*Rho1, *Sc*Rho3 and *Sc*Bem1, and with proteins of the late secretory system (Adamo et al., 1999; France et al., 2006; Guo et al., 2001; Zhang et al., 2001). Therefore, it constitutes an interface between cell polarity and the secretory pathway (Guo et al., 1999). Although the importance of polarized exocytosis in hyphal growth is undisputed, no systematic investigations have been performed in filamentous fungi. Only recently, it was described that the *A. nidulans* Sec3 homolog localizes to a narrow area at the hyphal tip (Taheri-Talesh et al., 2008) and that deletion of *CaSEC3* blocks formation of hyphae in *Candida albicans* (Li et al., 2007).

In order to understand hyphal morphogenesis, it is not only important to know the contribution of single factors but also how factors work together to form the machinery that governs polar growth. Therefore, we have begun to analyze the exocyst, cell polarity determinants and the polarisome in *A. gossypii* hyphae that elongate with different speeds. Mature hyphae grow up to 40 times faster than newly established hyphae, i.e. germ tubes and emerging lateral branches (Ayad-Durieux et al., 2000; Knechtle et al., 2003). We hypothesize that changes in growth speed would influence the localization or dynamics of components in the tip.

First, we report on light and electron microscopy experiments to search for a Spitzenkörper in hyphal tips of *A. gossypii*. Then we address the issues of whether all exocyst components are essential in *A. gossypii*, which area of the tip is associated with exocyst components and whether this area increases during acceleration of hyphal growth. We also asked whether key polarity factors and polarisome components localize to the exocyst area, whether the localization of these factors changes with increasing elongation speed, whether the localization of polarisome components depend on each other, and whether zones of exocytosis and endocytosis overlap or not. Finally, we test the role of the cytoskeleton for the distribution of exocyst and polarisome components.

Results

Formation of a Spitzenkörper in fast growing hyphae

Hyphal elongation speeds increase during the development of *A. gossypii*. Emerging hyphae of germlings elongate at about 0.2 µm/minute. Within 24 hours, hyphal growth speed accelerates to 3.5 µm/minute. Examples of slow and fast hyphae are shown in Fig. 1A. Interestingly, the diameter of hyphae changes with growth speed. Faster growth correlates with a hyphal diameter increase from around 3.5 to 5.0 µm (Fig. 1B). This implies that a doubling of growth speed leads to a more than twofold increase in surface expansion rate and explains the non-linear relationship between hyphal speed and surface expansion rate (Fig. 1C). New membrane and cell wall material is transported to sites of growth via secretory vesicles. The demand for delivery and processing of these vesicles in hyphal tips increases more than tenfold during acceleration of growth. Does this lead to other observable changes in addition to the described increase in hyphal diameters? If growth of fast hyphae is monitored by phase-contrast light microscopy on Ashbya full medium (AFM) solidified with gelatine, a dark apical body is observed in the tip dome (Fig. 1D). As expected, this area shows a strong accumulation of vesicles when analyzed by transmission electron microscopy (Fig. 1E). Two major classes of vesicles were observed with diameters of 20-40 µm and 80-100 µm, respectively (Fig. 1F). This corresponds well to the vesicle sizes reported for

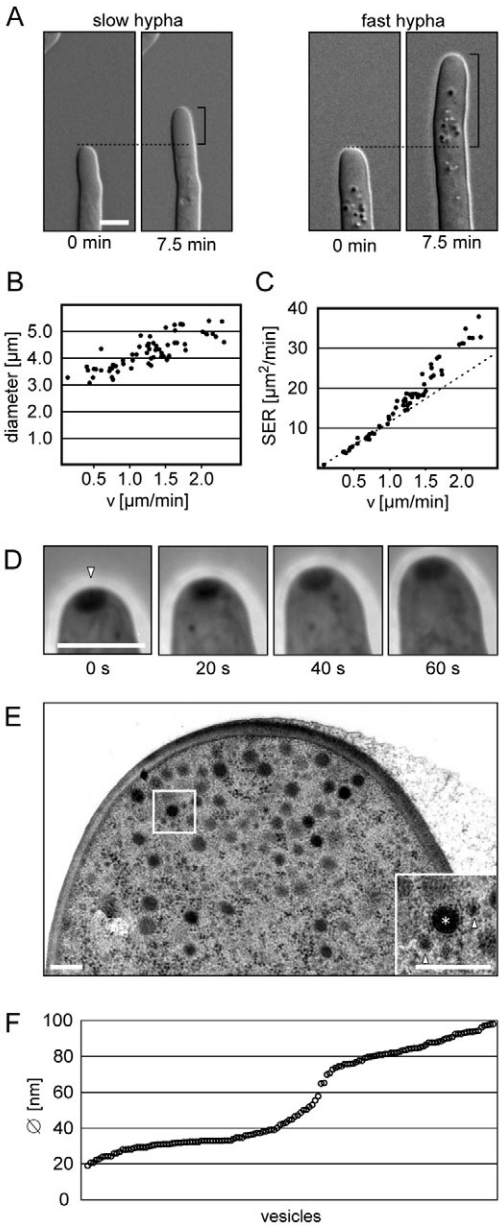

Fig. 1. Light and electron microscopy of *A. gossypii* hyphae. (A) Slow- and fast-growing hyphae. The square brackets indicate the section of the hyphae that grew for 7.5 minutes. (B) Hyphal diameters measured 5 µm behind the tip (*y*-axis) plotted against growth speed (*x*-axis). Mycelium from the border of a 3-day-old *A. gossypii* colony was inoculated on thin layer of AFM agar on microscopy slides at room temperature. Elongation speeds were determined as described in the Materials and Methods. (C) Surface expansion rate (SER, *y*-axis) plotted against growth speed (*x*-axis). The SER was determined as the product of hyphal circumference and growth speed. The circumference was calculated from the hyphal diameter assuming a circular hyphal profile. The broken line indicates the surface expansion rate of a (theoretical) hypha with a fixed diameter of 3.8 µm. (D) Spitzenkörper (white arrowhead) visible on AFM containing 19% gelatin. The numbers indicate time in seconds. The hyphae were covered with a cover slide and allowed to recover for 2 hours prior to imaging. Scale bars in A,D: 5 µm. (E) Transmission electron microscopy micrograph of 60 nm section of a cryofixed *A. gossypii* hyphal tip. The inset shows a higher magnification of the region enclosed by the rectangle. The white arrowheads depict small vesicles and the asterisk indicates a large vesicle. Scale bars: 400 nm. (F) The diameters of 140 tip-based vesicles were measured and plotted on the *y*-axis. The vesicle with the lowest diameter marks the left end of the *x*-axis, the vesicle with the biggest diameter indicates the right end.

Table 1. Exocyst components in *A. gossypii*

A. gossypii exocyst gene	*S. cerevisiae* exocyst gene*	ORF size (in amino acids) *A. gossypii*/*S. cerevisae*	Identity to *S. cerevisae* homolog	*A. gossypii* deletion
AgEXO70 (AFR100W)	ScEXO70 (YJL085W)	615/623	50%	Lethal
AgEXO84 (ADL321W)	ScEXO84 (YBR102C)	698/753	43%	Lethal
AgSEC10 (AGL130C)	ScSEC10 (YLR166C)	832/871	45%	Lethal
AgSEC15 (AFR252C)	ScSEC15 (YGL233W)	869/910	49%	Lethal
AgSEC3 (ADR012C)	ScSEC3 (YER008C)	1320/1336	33%	Lethal
AgSEC5 (AGL158C)	ScSEC5 (YDR166C)	860/971	43%	Lethal
AgSEC6 (ACL047W)	ScSEC6 (YIL068C)	793/805	52%	Lethal
AgSEC8 (ADL317C)	ScSEC8 (YPR055W)	977/1065	36%	Lethal

*Only one syntenic homolog of every *A. gossypii* exocyst component is present in *S. cerevisiae*.

other filamentous fungi (Harris et al., 2005; Steinberg, 2007). None of the inspected thin sections showed a fusion intermediate of a vesicle with the plasma membrane, most probably because vesicle fusions proceed very fast. Taken together, these data indicate that fast growing *A. gossypii* hyphae possess a Spitzenkörper. In slow hyphae, Spitzenkörper were not observed (as will be shown later).

Exocyst components localize to the cortex of the tip dome and take a spheroid shape in fast hyphae

Acceleration of hyphal growth and the concomitant increase of the surface expansion rate are only possible with an increased fusion rate of secretory vesicles. First, we wanted to know where these vesicles fuse with the plasma membrane, i.e. over the entire surface or only in a restricted area of the tip, and whether this area would enlarge with an increased demand for vesicle fusion. To address these issues, we analyzed the exocyst of *A. gossypii*. Homologs of the eight *S. cerevisiae* exocyst genes are present in the *A. gossypii* genome (Table 1). Individual deletions of the eight *A. gossypii* exocyst genes were lethal (Table 1), which is in agreement with the essential function of exocytosis in hyphal growth. We assessed the localization of GFP and YFP fusions to three exocyst components, *Ag*Exo70, *Ag*Sec3 and *Ag*Sec5 in hyphae elongating with different speeds. In slowly growing hyphae *Ag*Exo70-GFP localized as a cortical cap in the tip dome. At higher elongation speeds, it accumulated inside the hyphal tip finally taking a spheroid shape (Fig. 2A). For quantification, the expansion of the *Ag*Exo70-GFP signal parallel to the hyphal growth axis was plotted against the growth speed (Fig. 2B). The data points show that the size of the *Ag*Exo70-GFP signal gradually enlarges with increasing growth speed. Hyphal tips with cortical *Ag*Exo70-GFP caps elongated with less than 1.0 μm/minute. Tips with a spheroid *Ag*Exo70-GFP distribution extending about 1.2 μm along the hyphal axis grew faster than 1.4 μm/minute. Crescent-like localization were observed in hyphae with intermediate growth speeds (see examples marked a-c in Fig. 2A,B). Very similar localization, cortical caps at low speed and enlarging distributions up to spheroids with increasing growth speeds were observed for *Ag*Sec3-YFP (Fig. 2C,D) and *Ag*Sec5-GFP (data not shown). Thus, the localization of *Ag*Exo70-GFP, *Ag*Sec3-YFP and *Ag*Sec5-GFP in hyphal tips correlated closely with growth speed.

Colocalization of exocyst components and the Spitzenkörper in fast hyphae

We next tested whether the tip-based spheroid-shaped distribution of exocyst components observed in fast hyphae correlates with the dimensions of the Spitzenkörper shown in Fig. 1D. The gelatine-enriched medium that allows resolution of intracellular details showed strong background fluorescence. Therefore, we used the lipophilic dye FM4-64, which stains the Spitzenkörper in different fungal species most probably owing to fast recycling of endocytosed membrane material in the tip region (Fischer-Parton et al., 2000). In *A. gossypii*, FM4-64 accumulation in the Spitzenkörper became apparent between 2.7 and 5.5 minutes after dye addition (n=9), whereas staining of putative vacuoles was visible only after prolonged incubations (see Fig. S1 in the supplementary material). Interestingly, fast but not slow *A. gossypii* hyphae accumulated FM4-64 in a spherical region in the tip (Fig. 3A,B). The spherical region stained with FM4-64 overlapped with the spherical localization of *Ag*Exo70-GFP, *Ag*Sec3-YFP (Fig. 3C) and *Ag*Sec5-GFP (data not shown). No FM4-64-stained Spitzenkörper could be detected at growth speeds at which exocyst components were exclusively observed as cortical caps (Fig. 2; Fig. 3B). Together, these observations strongly suggest that, in fast hyphae, exocyst components are part of the Spitzenkörper. Furthermore, not only Spitzenkörper localization of exocyst components but Spitzenkörper formation itself depends on hyphal growth speed.

*Ag*Cdc42, *Ag*Cdc24 and *Ag*Bem1 do not localize to the Spitzenkörper

We wondered whether the exocyst is active at the cortical cap and in the Spitzenkörper region. To answer this question, we localized *A. gossypii* homologs of budding yeast proteins, which are known to promote exocytosis by interacting with the exocyst. Among them were homologs of the conserved GTP-binding protein *Sc*Cdc42 and the adaptor protein *Sc*Bem1 (France et al., 2006; Zhang et al., 2001). A functional *GFP-AgCDC42* fusion was obtained using a novel, selection-based screening approach (described in the Materials and Methods). As the exocyst interacts with Cdc42 in its GTP-bound active state (Zhang et al., 2001), we additionally localized *Ag*Cdc24, the putative guanine nucleotide exchange factor for *Ag*Cdc42 (Wendland and Philippsen, 2001). Strikingly, GFP-*Ag*Cdc42, *Ag*Cdc24-GFP and *Ag*Bem1-GFP localized as cortical caps only to the tip dome, even in fast hyphae that displayed an FM4-64-stained Spitzenkörper (Fig. 4). This strongly indicates that *Ag*Cdc42 interacts with the exocyst at the cortex, where exocytosis most likely takes place. The GFP-fluorescence in the Spitzenkörper probably represents exocyst components that are associated with vesicles, because in yeast, all the exocyst components, except Sec3, are associated with secretory vesicles (Boyd et al., 2004; Guo et al., 1999).

The exocyst cap in the tip dome continuously shrinks and expands

We examined tips of fast hyphae (extension rate >1.50 μm/minute) displaying a spheroid *Ag*Exo70-GFP distribution. Additionally to

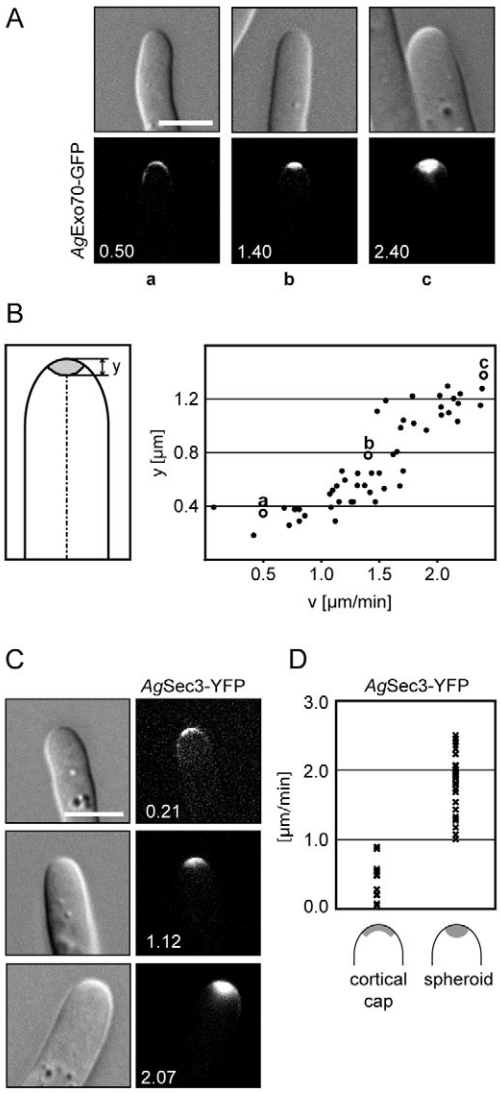

Fig. 2. The localization of exocyst components depends on growth speed. (A) *Ag*Exo70-GFP in hyphal tips (central planes of *z*-series). The white numbers indicate growth speed in µm/minute. (B) Growth speed and *Ag*Exo70-GFP localization. The dimensions of the *Ag*Exo70-GFP signals (y) were measured as shown in the sketch and plotted against growth speed in µm/minute (v). Micrographs for the data-points labeled 'a', 'b' and 'c' in A. (C) *Ag*SEC3-YFP expressing hypha. Growth speed is indicated in µm/minute. (D) Simplified speed/localization plot. Growth speeds are given in µm/minute on the *y*-axis. The two different localization patterns are shown on the *x*-axis. Growth speeds of hyphae that displayed a cortical *Ag*Sec3-YFP localization are shown on the left half of the plot, growth speeds of hyphae with a spherical *Ag*Sec3-YFP localization are shown on the right half. Hyphae that displayed a crescent-like *Ag*Sec3-YFP localization were not considered in this analysis. Scale bars: 5 µm.

the Spitzenkörper-based *Ag*Exo70-GFP pool, a pronounced cortical *Ag*Exo70-GFP cap was observed (Fig. 5A). This cortex-associated *Ag*Exo70-GFP most probably indicates the zone where the exocyst promotes secretory vesicle fusion with the plasma membrane. As stated above, the increasing surface expansion rates that occur during hyphal acceleration demand an increase in fusion of secretory vesicles. A way to increase the fusion rate would be to expand the area where vesicle fusion happens. To test whether this is the case, we measured the area of the cortical *Ag*Exo70-GFP cap and compared it with the hyphal growth speed (Fig. 5B). Interestingly, the sizes of this area ranged from 5 to 15 µm^2, without any clear indication of a much larger cortical exocyst area at higher growth speeds. The greater than tenfold increase in surface expansion rate that is observed during hyphal acceleration (Fig. 1C) is thus not mediated by a substantial expansion of the apical vesicle fusion zone. Consequently, compared with slow hyphae, exocytosis has to be much more efficient in a restricted area at the cortex of fast growing hyphal tips. Though no correlation with growth speed was found, the cortical area of *Ag*Exo70-GFP enrichment was quite variable. We thus wanted to test whether this variability reflects normal fluctuations over short times or whether hyphae display slowly changing apical vesicle fusion zones of different sizes. We monitored the *Ag*Exo70-GFP distribution in time-lapse movies (Fig. 5C; see Movie 1 in the supplementary material). Within the 60 seconds that are covered by this movie, the apical vesicle fusion zone enlarged from 10 µm^2 to over 15 µm^2 and shrunk again to 10 µm^2 (Fig. 5D). During this time period, hyphal growth speed did not change (Fig. 5D). The *Ag*Exo70-GFP marked Spitzenkörper stayed at its position in the hyphal apex, although its shape was changing constantly (Movie 1). Even though, size and position of the vesicle fusion zone as well as the shape of the Spitzenkörper fluctuate, on average they are centered on the growth axis (Fig. 5E).

The polarisome components *Ag*Spa2 and *Ag*Pea2 and the formin *Ag*Bni1 localize to the Spitzenkörper, whereas *Ag*Bud6 is restricted to the cortex

Another complex involved in polar surface expansion is the polarisome, a poorly defined network of interacting proteins that was mainly studied in budding yeast (Park and Bi, 2007). It consists of *Sc*Spa2, *Sc*Pea2 and *Sc*Bud6 (Sheu et al., 1998). As *Sc*Spa2 and *Sc*Bud6 are involved in the localization and regulation of the formin *Sc*Bni1, the latter is often considered to be a fourth member of the polarisome (Evangelista et al., 1997; Fujiwara et al., 1998; Moseley et al., 2004). The *A. gossypii* genome encodes homologs for all four proteins. Loss of the formin *Ag*Bni1, which mediates the formation of the actin cables, is lethal (Schmitz et al., 2006). Deletion mutants of *AgSPA2* are viable but hyphae elongate with decreased speed (Knechtle et al., 2003). Similarly, we found reduced growth rates for *Agpea2Δ* and *Agbud6Δ* strains. Radial growth speeds were 1.1 µm/minute, about one-third of wild-type mycelium on AFM at 30°C (Fig. 6A; Table 2). This similar reduction in maximal hyphal elongation indicates an important role for the polarisome components to reach fast growth. We wanted to test whether the role of the three non-essential polarisome proteins for fast growth is reflected by their tip localization. We also included AgBni1 in this analysis. In slow growing hyphae, fusions of polarisome components to GFP or YFP localized to the tip cortex (Fig. 6B,C), as was the case for the exocyst components or cell polarity factors. This finding suggests that all the polarisome components also function in hyphal growth at lower growth speeds. In fast hyphae, GFP-*Ag*Bni1, *Ag*Spa2-GFP and *Ag*Pea2-YFP were observed in a spherical localization (Fig. 6B,C). Crescent-shaped localization were observed at intermediated growth speeds (Fig. 6B). FM4-64 staining revealed that *Ag*Spa2-GFP, *Ag*Pea2-YFP and GFP-*Ag*Bni1 localize to the Spitzenkörper (Fig. 6D). By contrast, GFP-*Ag*Bud6 was restricted to the cortex independent of growth speed (Fig. 6B,C) even though an FM4-64-stained Spitzenkörper was observed (Fig. 6D). The localization of the polarisome components overlap only at the cortex of the hyphal tip. Therefore, a hypothetical protein

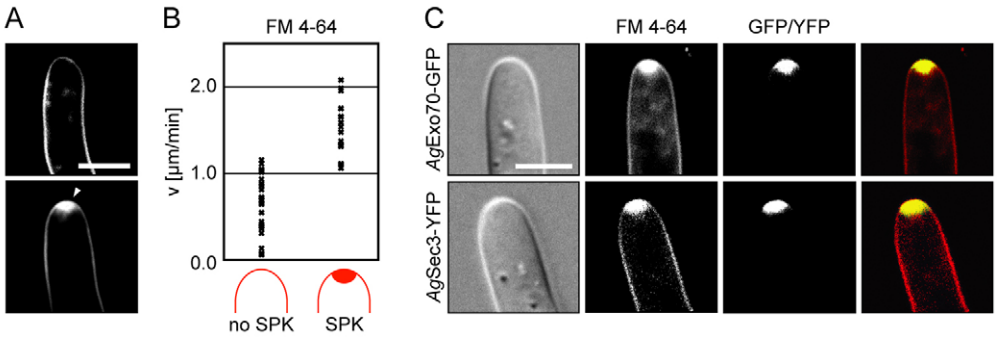

Fig. 3. Exocyst components localize to the *A. gossypii* Spitzenkörper. (A) FM4-64-stained hyphal tips. The arrowhead indicates an FM4-64-stained Spitzenkörper that is observed in some hyphae. (B) Correlation between growth speed and FM4-64-stained Spitzenkörper. Growth speeds of hyphae without accumulation of internal FM4-64 fluorescence in the hyphal tip are plotted on the left side of the graph; growth speeds of hyphae with a Spitzenkörper are plotted on the right side. (C) FM4-64 staining (red in the overlay) of an *AgEXO70-GFP* and an *AgSEC3-YFP* hypha (green in the overlay). Overlaps appear yellow. Scale bars: 5 µm.

complex containing all four polarisome components could exist only at the cortex.

In fast hyphae GFP-*Ag*Bni1 was not present in the entire Spitzenkörper like *Ag*Exo70-GFP and *Ag*Spa2-GFP (Fig. 3C; Fig. 6D upper panels). We tested potential differences in the distribution of these proteins by employing three-dimensional deconvolution of image stacks of 32 planes each. For each strain, 30 hyphal tips growing faster than 1.50 µm/minute were analyzed. We found that the localization of GFP-*Ag*Bni1, *Ag*Spa2-GFP and *Ag*Exo70-GFP differed from each other. In 71% of all cases, GFP-*Ag*Bni1 was enriched in a small spot in the tip dome (Fig. 6E, black arrowhead). In the remaining 29% GFP-*Ag*Bni1 either was homogenously distributed in the Spitzenkörper or localized in a large, fuzzy core region that was connected to the cortex (not shown). Furthermore, a zone of reduced GFP-*Ag*Bni1 fluorescence at the very tip proximal to the core-region was observed in 58% of all cases (Fig. 6E, grey arrowhead). Similar to GFP-*Ag*Bni1, *Ag*Spa2-GFP was enriched in a small spot in 52% of all tips though the fluorescence intensity difference between the spot and the surrounding *Ag*Spa2-GFP signal was less pronounced (Fig. 6F, arrowhead). In 34% of the hyphae, *Ag*Spa2-GFP displayed a uniform Spitzenkörper-like localization (Fig. 6F, bottom row), the remaining 14% displayed irregular or crescent-like *Ag*Spa2-GFP localization (not shown). Enrichment of *Ag*Exo70-GFP in a central spot was not observed (Fig. 5A).

Localization of polarisome components in deletion strains

In order to test whether the localization of polarisome components depend on each other, we deleted the three non-essential polarisome genes in the strains with fluorescently labeled polarisome components. The mutant strains displayed hyphal diameters significantly larger than the wild type (Fig. 6G; Table 2). Fluorescently labeled polarisome components still localized to hyphal tips in the deletion strains, except *Ag*Pea2-YFP in *Agspa2Δ* (Fig. 6G; see Fig. S2 in the supplementary material). In some deletions, the fluorescence intensity at the tip was weaker than in wild-type strains. This most probably indicates a diminished recruitment to the tip, as expression of the fluorescently labeled polarisome components was not affected by the deletions (see Fig. S2 in the supplementary material). In all deletion strains, GFP-*Ag*Bni1, *Ag*Spa2-GFP and *Ag*Pea2-YFP were restricted to the cortex of the tip dome. This was not only due to the low growth speeds inflicted by the mutations, as polarisome components frequently showed crescent-shaped localization patterns in wild-type hyphae with comparable speeds (Fig. 6G; see Fig. S2 in the supplementary material). For quantification, the ratio between the maximal fluorescence value in the tip and 10 µm subapical to the tip was determined (Fig. 6H). In summary, deletion of either *AgSPA2* or *AgPEA2* resulted in very strong reduction or loss of the tip localization of GFP-*Ag*Bni1, *Ag*Spa2-GFP or *Ag*Pea2-YFP. These findings are consistent with the localization data in such that all the factors found in the Spitzenkörper also strongly depend on each other for localization. Although the fluorescence reduction was less pronounced, the GFP-*Ag*Bud6 localization was affected in *Agspa2Δ* and *Agpea2Δ* strains, and, vice versa, the localization of *Ag*Spa2-GFP and *Ag*Pea2-GFP was affected in the *Agbud6Δ* strain. Strikingly, the maximal GFP-*Ag*Bni1 fluorescence in the tip was not decreased in *Agbud6Δ*, indicating that *Ag*Bni1 does not depend on *Ag*Bud6 for its concentration at sites of polar growth. Similar dependencies between polarisome components are described in budding yeast. *Sc*Spa2 and *Sc*Pea2 play an important role for recruitment of *Sc*Bni1, *Sc*Spa2 and *Sc*Pea2 (Fujiwara et al., 1998; Ozaki-Kuroda et al., 2001; Sheu et al., 1998; Valtz and Herskowitz, 1996), whereas lack of *Sc*Bud6 only slightly disturbs *Sc*Bni1 localization (Jin and Amberg, 2000; Ozaki-Kuroda et al., 2001). Thus, in both *A. gossypii* and budding yeast, Bni1, Spa2 and Pea2 seem to form a functional unit. These proteins interact together in

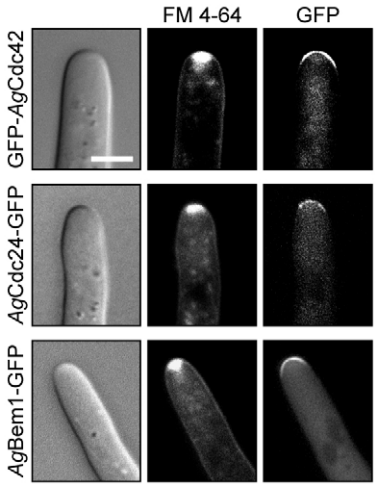

Fig. 4. Cell polarity factors localize to the cortex tip. DIC and fluorescence images of *GFP-AgCDC42*, *AgCDC24-GFP* and *AgBEM1-GFP* hyphae stained with FM4-64. Scale bar: 5 µm.

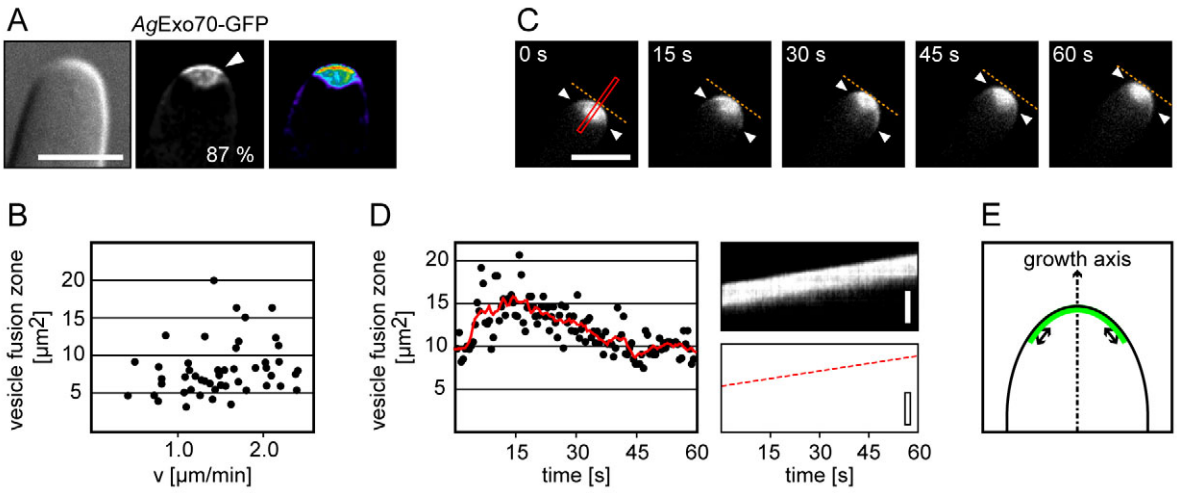

Fig. 5. Size variations of cortical *Ag*Exo70-*GFP* caps. (A) A *z*-series of *AgEXO70-GFP* hypha that grew faster than 1.50 µm/minute was subjected to blind deconvolution. Maximum projections of central planes are shown. Red in the false-colored image indicates high GFP-fluorescence intensity, blue and purple indicate low intensity. Eighty-seven percent of the hyphae showed an accumulation of *Ag*Exo70-GFP at the cortex (arrowhead, *n*=31). (B) The sizes of the cortical *Ag*Exo70-GFP areas were estimated assuming that the arc-shaped fluorescent zone visible in the central plane represents the central section of a spherical cap. These values (*y*-axis) were plotted against growth speed. (C) Frames from time-lapse Movie 1 of an *AgEXO70-GFP* hypha. The broken lines indicate the hyphal tip, the arrowheads indicate the border of the vesicle fusion zone. Scale bars for A,C: 5 µm. (D) The area of the vesicle fusion zone was estimated for every frame of Movie 1 and plotted against time. The red line results from plotting the mean vesicle fusion area for every 4-second interval. The kymograph shows GFP fluorescence enclosed by the red rectangle in D over time. The advancing tip front is indicated with a broken line. The constant slope of this line indicates a constant growth speed. Scale bars: 2 µm. (E) Model for the size variations of cortical *Ag*Exo70-GFP caps.

budding yeast, they localize to the Spitzenkörper in *A. gossypii* and loss of one of these proteins affects the localization of the other two in both *S. cerevisiae* and *A. gossypii*.

Role of the cytoskeleton in mediating Spitzenkörper integrity

Formins and f-actin are found in the hyphal tip region of different fungi, including *A. gossypii* (Bourett and Howard, 1991; Crampin et al., 2005; Harris et al., 2005; Schmitz et al., 2006; Srijayanthi et al., 1996; Taheri-Talesh et al., 2008). This led to the speculation that formin-mediated actin cables are responsible for Spitzenkörper integrity and tip growth by clustering and redistributing secretory vesicles that are transported on microtubules to the tip region (Harris et al., 2005). To test whether this model is applicable to *A. gossypii*, we treated growing hyphae with either nocodazole or latrunculin A to disrupt microtubules or f-actin, respectively. Our results confirmed findings that *A. gossypii* hyphae continue to elongate in the presence of nocodazole, indicating that efficient transport of secretory vesicles from subapical regions does not depend on cytoplasmic microtubules (Fig. 7A) (Gladfelter et al., 2006). On the other hand, disruption of the actin cytoskeleton leads to swelling of hyphal tips and lysis within 15 minutes (Fig. 7B) (Knechtle et al., 2006), confirming the essential role of F-actin in tip growth of filamentous fungi (Akashi et al., 1994; Torralba et al., 1998).

It has been reported that disruption of microtubules leads to reduced hyphal elongation rates (Fuchs et al., 2005; Horio and Oakley, 2005). Therefore, microtubules may be important for fast hyphal elongation in *A. gossypii*. To test this, the growth speed of nocodazole-treated and untreated hyphae was monitored in time-lapse movies (Fig. 7C). Nocodazole-treated hyphae extended with 2.7±0.2 µm/minute, which was similar to the mock-treated cells that grew with 2.9±0.2 µm/minute. A spherical *Ag*Exo70-GFP localization was still observed in 72% of hyphal tips 15 minutes after nocodazole administration (Fig. 7D), thus the Spitzenkörper-like distribution of *Ag*Exo70-GFP was only marginally influenced by the loss of microtubules.

In order to further characterize the role of actin in tip growth, we assessed the localization of *Ag*Exo70-GFP and *Ag*Spa2-GFP in hyphae stained with Alexa568-phalloidin, which strongly labels the tip-enriched actin patches and, less intensely, actin cables (Fig. 7E,F). The staining shows a separation of the zone of exocytosis, indicated by *Ag*Exo70-GFP, and endocytosis, indicated by the dense area of actin patches (Huckaba et al., 2004; Kaksonen et al., 2003). It seems that the faster the hyphae elongate, the more the endocytic zone is shifted away from the tip (data not shown). Two to six faint actin cables could be observed subapically of the endocytic zone. Whether these cables extended into the tip or not could not be determined due the intense fluorescence of the actin patches. The integrity of the tip-localized *Ag*Exo70-GFP and *Ag*Spa2-GFP pools were assayed by incubation of the hyphae with 200 µM latrunculin A. Only traces of cortical f-actin remained after 60 seconds and no f-actin staining was detected after 180 seconds of drug treatment. The spheroid-shaped *Ag*Exo70-GFP localization disappeared after 15 seconds in most of the hyphae, whereas the cortical *Ag*Exo70-GFP population persisted (Fig. 7G,H). The *Ag*Spa2-GFP signal lost its spheroid shape after 15 seconds but two distinct areas of localization of *Ag*Spa2-GFP were observed: a cortical cap and a dense spot that was observed in the proximity of the cortex (Fig. 7I,J). This spot may represent the dislocalized intense spot seen in the central Spitzenkörper region, potentially indicating a structural integrity of this spot. In a similar way, GFP-*Ag*Bni1 was found in a bright spot additional to the cortical cap after 60 seconds of latrunculin A treatment (data not shown). These observations suggest that cortex-associated pools of the investigated proteins are maintained in an actin-independent way, whereas the Spitzenkörper pool is very sensitive to perturbation of the actin cytoskeleton.

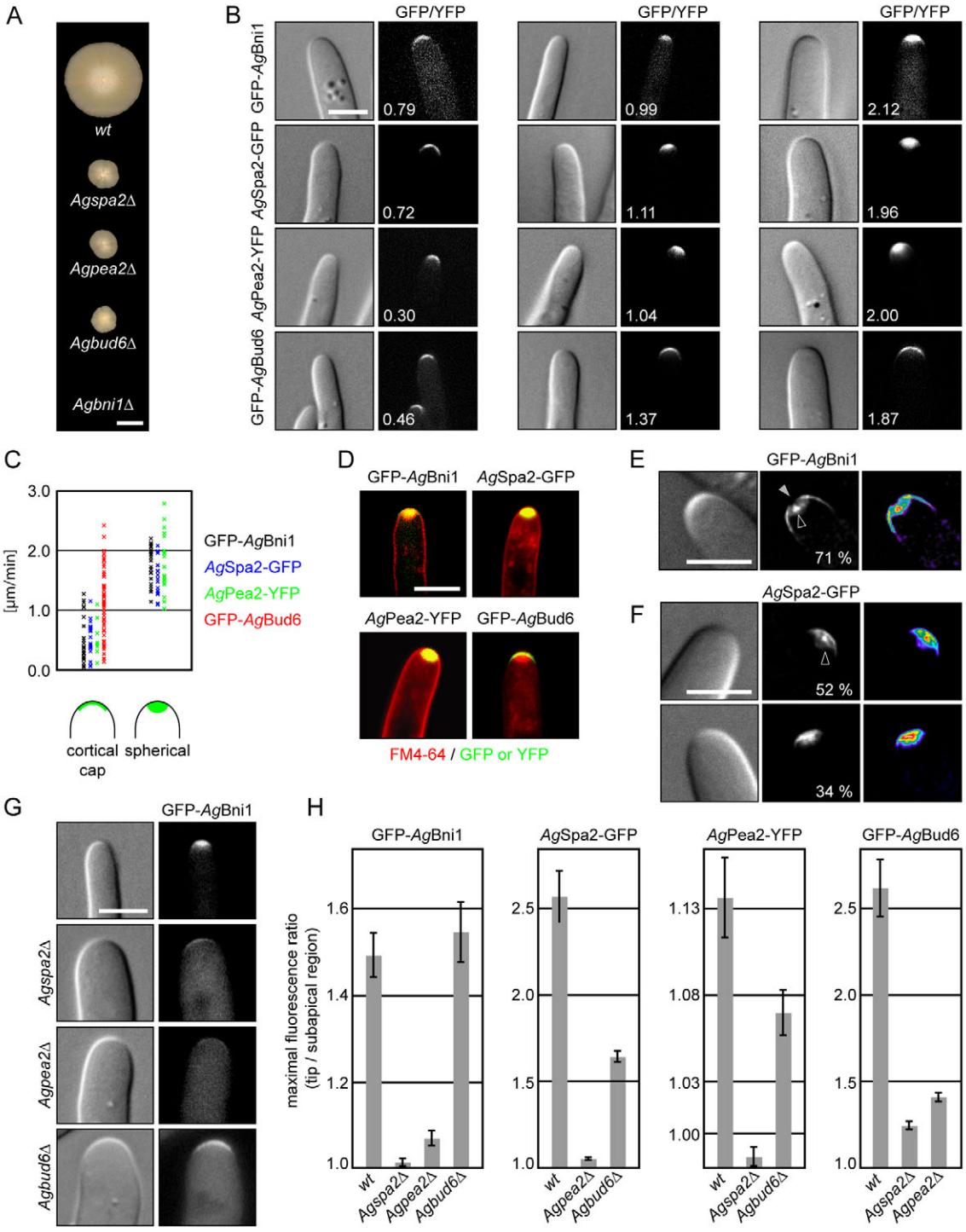

Fig. 6. The polarisome components *Ag*Spa2 and *Ag*Pea2 and the formin *Ag*Bni1 localize to the Spitzenkörper at high growth speeds. (A) Radial growth of polarisome deletion strains. Mycelium of *wt*, *Agspa2Δ*, *Agpea2Δ* and *Agbud6Δ* was inoculated on AFM agar, spores of a heterokaryonic *Agbni1Δ* strain were spotted on selective medium and incubated for 6 days at 30°C. Scale bar: 2 cm. (B) DIC and fluorescence images of *GFP-AgBNI1*, *AgSPA2-GFP*, *AgPEA2-YFP* and *GFP-AgBUD6* hyphae. The white numbers indicate growth speed in µm/minute. (C) Correlation between localization and growth speed of the polarisome components. Growth speeds are plotted on the *y*-axis in µm/minute, the localization of the GFP- or YFP-tagged proteins are shown on the *x*-axis. (D) Overlay of fluorescently labeled polarisome components (green) and FM4-64 staining (red). (E) Stacks of GFP-*Ag*Bni1-expressing hypha that grew faster than 1.50 µm/minute were subjected to blind deconvolution. Maximum projections of central planes are shown. Seventy-one displayed a core-like localization of GFP-*Ag*Bni1 (black arrowhead, *n*=31). The gray arrowhead indicates a zone of reduced GFP-*Ag*Bni1 fluorescence. (F) Deconvoluted fluorescence images of *AgSPA2-GFP* hyphae. Fifty-two percent of fast hyphae displayed an enrichment of *Ag*Spa2-GFP in a core region in the Spitzenkörper (top row, black arrowhead). Thirty-four percent of the hyphae displayed a uniform Spitzenkörper localization (bottom row, *n*=29). (G) GFP-*Ag*Bni1 in polarisome deletion strains. The hyphae grew with speeds of between 0.9 and 1.1 µm/minute. (H) Fluorescence ratios between the tip and the cytoplasm. Maximal GFP or YFP fluorescence was determined in two circular areas of 5 µm diameter, the centers of which were located in the tip and in the cytoplasm 10 µm away from the tip. The average ratios tip/cytoplasm were plotted. More than 15 hyphae with a growth speed between 0.75 and 1.3 µm/minute were assessed per strain. Error bars indicate s.e.m. Scale bars for B,D-G: 5 µm.

Table 2. Deletion of polarisome genes

A. gossypii strain	Radial growth speed ± s.e.m. (μm/minute)*	Hyphal diameter ± s.e.m. (μm)†
Wild type	3.44±0.02	5.0±0.1
Agspa2Δ	1.11±0.02	6.5±0.1
Agpea2Δ	1.10±0.01	6.2±0.1
Agbud6Δ	1.03±0.01	5.6±0.1
Agbni1Δ	Lethal	Lethal

*The radial growth of mycelia on AFM agar was followed for 7 days; n=4 for each strain.
†The hyphal diameter was measured in fast-growing hyphae 5 μm behind the tip; n>30 for each strain.

Discussion

The fungus *A. gossypii* is a well-suited biological system in which to study sustained polar surface expansion. Its genome carries at syntenic positions the homologs for all *S. cerevisiae* genes that encode known polarity components. Despite this conservation at the genome level, *A. gossypii* exclusively grows in the form of fungal hyphae (sustained polar surface expansion), whereas *S. cerevisiae* proliferates by alternating cycles of bud growth (mainly non-polar surface expansion) and cell separation. The biosynthetic capacity for surface growth also differs between both organisms. The tip surface of *A. gossypii* hyphae can extend up to 50 times faster than the surface of a growing yeast bud. It is therefore not surprising that we found distinct differences associated with cell surface growth in both systems, even though the basic function of individual polarity factors, mainly known from studies in *S. cerevisiae* (Park and Bi, 2007), was maintained during evolution.

It is well established that many polarity factors only transiently localize to tips of growing buds of *S. cerevisiae* and that polarized localization is not maintained during the non-polar growth phase, as shown for *Sc*Bni1 (Ozaki-Kuroda et al., 2001). Our studies indicate an intimate association between permanent tip localization of polarity factors and sustained polar growth of *A. gossypii* hyphae. We further show that the shape of the tip localization correlates with growth speed. At slow speeds, the exocyst, cell polarity factors and polarisome components form a cap at the tip cortex (Fig. 8A). With increasing growth speeds, the exocyst and three of the four polarisome components gradually accumulated, additionally to the cortical cap, in the tip dome (Fig. 8B). Electron microscopy showed that vesicles accumulate in this region. A substantial part of these are secretory vesicles as GFP-*Ag*Sec4 assumes a spheroid-shaped localization in hyphal tips (Schmitz et al., 2006). It is also likely that endocytosis-derived vesicles participate in this vesicle pool as FM4-64, a lipid dye that is taken up via endocytosis, accumulates within a few minutes in tips of fast hyphae (see Fig. S1 in the supplementary material).

Our findings represent compelling evidence that fast, but not slow, *A. gossypii* hyphae form a Spitzenkörper. A vesicle reservoir is apparently needed in tips of fast hyphae to coordinate and satisfy the increased demand for vesicle fusion (Fig. 8C). The finding that a Spitzenkörper is not present at slow growth speeds in *A. gossypii* suggests that this structure is not necessary for hyphal growth per se. This is supported by observations in *A. nidulans* where Spitzenkörper localization of a v-SNARE was observed in mature hyphae but not in slowly growing germlings (Horio and Oakley, 2005; Taheri-Talesh et al., 2008). Furthermore, slow expansion rates may explain the absence of a Spitzenkörper in *S. cerevisiae* buds or in *C. albicans* buds and pseudohyphae (Crampin et al., 2005).

Our data indicate that the Spitzenkörper forms gradually when hyphal growth speed accelerates. At intermediate growth speeds, we observed crescent-like localization of exocyst or polarisome components that seem to represent intermediate states between cortical and Spitzenkörper localization. It is obvious that the output of the secretory pathway has to increase to reach faster hyphal elongation rates. A more active secretory system may lead to gradual accumulation of vesicles in the tip. Along with the increase in local vesicle concentration, the efficiency of vesicle fusion with the plasma membrane will increase until a new steady state between vesicle transport and consumption is reached (Fig. 8C).

Even the fastest hyphae seem to carry an excess of vesicles in their tips, thus most probably excluding subapical vesicle supply as control for maximal growth speed. It is conceivable that maximal polar surface expansion depends on the capacity for docking and fusion of secretory vesicles at the tip cortex. The cortical vesicle fusion zone is defined by the localization of the exocyst and its activating factors. The size of this zone varied among hyphae of similar speed owing to its dynamic nature. Time-lapse movies showed that it was restricted to the very tip with fluctuating rims (Fig. 5). Remarkably, the average cortical area for vesicle fusion increases only slightly during the observed tenfold increase in surface expansion. Thus, vesicle fusion is spatially restricted. When the maximal fusion rate is reached in the confined tip area, hyphal growth speed may not increase further.

In *A. gossypii*, actin patches, which most probably represent sites of endocytosis, are excluded from the exocytic zone at the very tip. By contrast, they are evenly distributed at the cortex of growing yeast buds (Kaksonen et al., 2003). As long as buds are expanding, one has to assume that sites of exocytosis and endocytosis co-exist at the bud surface. In hyphal tips of *A. gossypii* actin patches are absent from the tip zone where the polarisome localizes (Knechtle et al., 2003) and also from the zone of exocytosis in fast growing hyphae. Therefore, zones of exocytosis and endocytosis do not overlap in *A. gossypii* hyphal tips. In contrast to slow hyphae, the zone of endocytosis is shifted further away from the tip front in fast growing hyphae (Fig. 8D).

The proteins assessed in this study can be divided into two groups: proteins that localize to the cortex and the Spitzenkörper; and proteins that are restricted to the cortex. Exocyst components as well as the polarisome components *Ag*Spa2, *Ag*Pea2 and *Ag*Bni1 accumulated in the Spitzenkörper, which mainly consists of vesicles. This localization pattern was not surprising for the exocyst components *Ag*Exo70 and *Ag*Sec5 as their budding yeast homologs are transported with secretory vesicles. Furthermore, there is also evidence that *Sc*Spa2 associates with secretory vesicles (Shih et al., 2005), which could explain the localization of *Ag*Spa2 to the Spitzenkörper. However, no association between *Sc*Pea2 and *Sc*Sec3 with vesicles was observed in similar assays (Boyd et al., 2004; Shih et al., 2005). Thus, there are two alternative explanations for the Spitzenkörper localization of these proteins in *A. gossypii*. It is possible that *Ag*Pea2 and *Ag*Sec3 associate with an ill-defined matrix in the Spitzenkörper region,

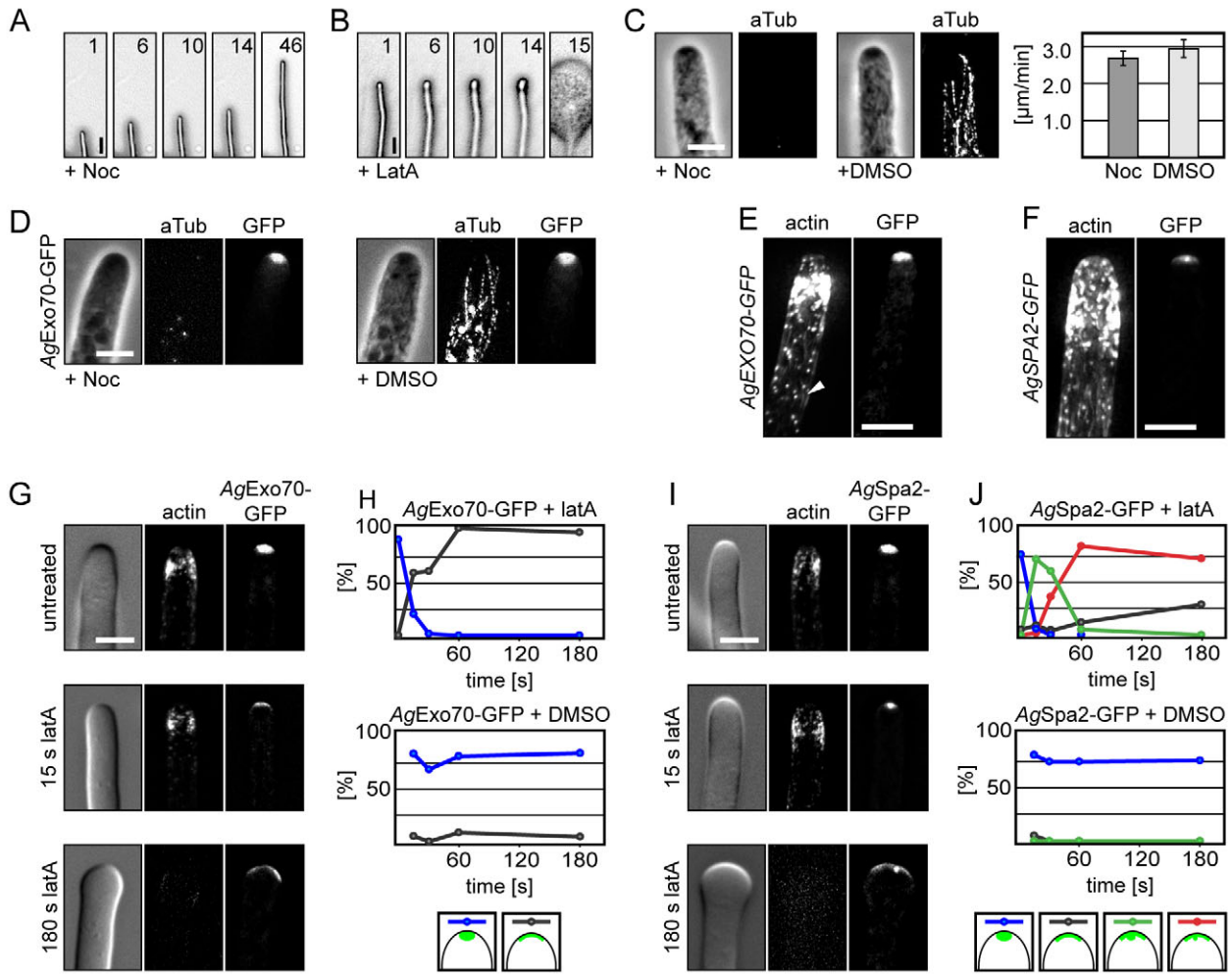

Fig. 7. Disruption of the microtubule and the actin cytoskeleton in fast-growing hyphae. Hyphal growth after addition of (A) 30 µg/ml nocodazole or (B) 400 µM latrunculin A. The drugs were pipetted onto the border of a 2-day-old mycelium on AFM agar. The numbers indicate the time after drug addition in minutes. Scale bars: 20 µm. (C) Growth speed of hyphae treated with 15 µg/ml nocodazole. Micrographs show anti-tubulin staining (aTub) of nocodazole- or DMSO-treated hyphae prior to the growth speed assessments. The 20-hour-old mycelia were treated with nocodazole for 2 minutes and transferred to solid medium containing nocodazole. Three movies were acquired per condition and the speed of 10 hyphae was measured per movie. Error bars=s.e.m. (D) Immunofluorescence staining of microtubules (aTub) in *AgEXO70-GFP*. Mycelia were grown and treated as above. Actin staining of *AgEXO70-GFP* (E) and *AgSPA2-GFP* (F) grown for 20 hours in liquid AFM. The faint actin cables (arrowhead) are visible only in a subapical region of an overexposed micrograph owing to the clustered actin patches in the tip. (G) Latrunclin A treatment of *AgEXO70*-GFP. Samples were fixed prior to and 15, 30, 60 and 180 seconds after drug addition and stained with Alexa568-phalloidin. Micrographs of three time points are shown. (H) Quantification of characteristic *Ag*Exo70-GFP localization patterns observed upon latrunculin A-treatment. Forty to sixty hyphae were analyzed for the latrunclin A-treated samples and more than 20 for the DMSO controls. Schemes of the different localization patterns are shown below the graphs. The different categories do not add up to 100% as a few hyphae that displayed crescent-like or aberrant localization were not included. (I) Images of *AgSPA2-GFP* hyphae treated with latrunculin A as described in F. (J) Quantification of *Ag*Spa2-GFP localization in latrunculin A-treated samples. Scale bars for C-G,I: 5 µm.

but not with vesicles. Alternatively, *Ag*Pea2 and *Ag*Sec3 may, unlike their homologs in yeast, associate with vesicles directly or indirectly in *A. gossypii*. Such an association may not be needed in the relatively small *S. cerevisiae* cells, but may be necessary for long-distance transport in *A. gossypii* hyphae.

Other factors were restricted to the cell cortex, among them *Ag*Cdc42 and *Ag*Bud6. Interestingly, *Sc*Cdc42 and *Sc*Bud6 seem to be associated with vesicles in budding yeast and their localization depends on a functional secretory pathway (Jin and Amberg, 2000; Wedlich-Soldner et al., 2003; Zajac et al., 2005). Consequently, one would expect to find these factors in the Spitzenkörper in *A. gossypii*, which is not the case. There are two non-exclusive explanations for this observation. First, it is not known whether different types of secretory vesicles defined by their cargo exist in *A. gossypii* or whether all vesicles destined for fusion with the tip plasma membrane accumulate in the Spitzenkörper. It is thus possible that vesicles transporting *Ag*Cdc42 or *Ag*Bud6 do not accumulate or are too rare to be detected. Second, both *Sc*Cdc42 and *Sc*Bud6 are able to localize to sites of polar growth independently of actin in yeast, which suggests alternative localization mechanisms that do not depend on targeted vesicle transport (Ayscough et al., 1997). Similar mechanisms could be responsible for localization of *Ag*Cdc42 and *Ag*Bud6 to the tip cortex of *A. gossypii*.

*Ag*Bni1 is concentrated at the tip cortex and in the centre of the Spitzenkörper. Cdc42 binds to and activates Bni1 both in *S. cerevisiae* and *A. gossypii* (Evangelista et al., 1997; Schmitz et al.,

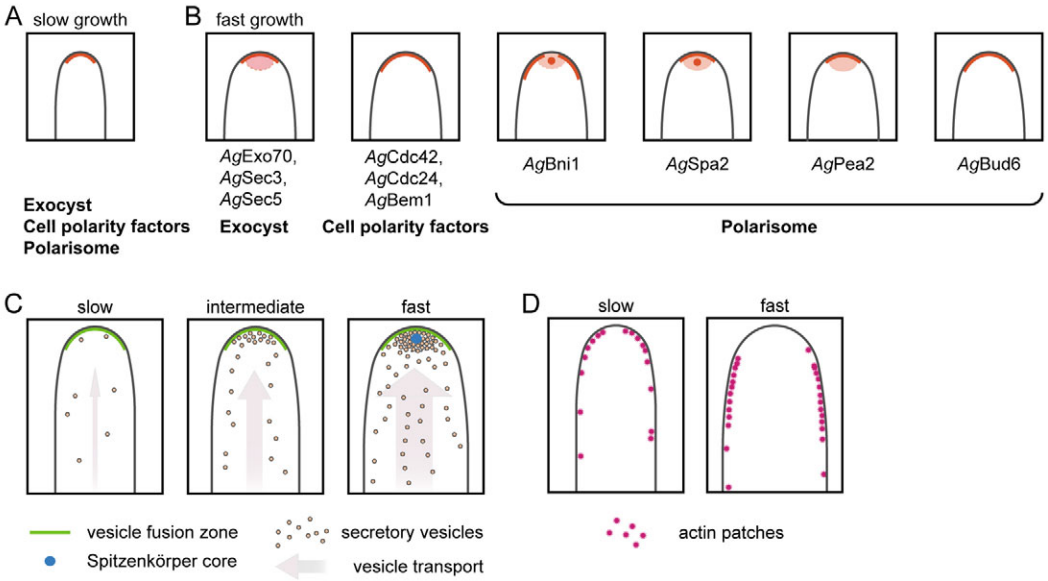

Fig. 8. A model for Spitzenkörper formation in *A. gossypii*. (A) A slow-growing hyphal tip is outlined, localization of the proteins listed below the sketch are shown in red. (B) Localization of the same proteins as in A in fast growing hyphae. (C) A model for Spitzenkörper formation. The relative amount of vesicle transport is symbolized by the width of the gray arrows. (D) Actin patches representing sites of endocytosis in slow and fast hyphae. In slow hyphae the tip front lacks actin patches (Knechtle et al., 2003). An extended tip zone lacks actin patches in fast hyphae (Fig. 7E).

2006). Furthermore, the actin polymerization activity of *Sc*Bni1 is stimulated by binding of the conserved *Sc*Bud6 C-terminal half in budding yeast (Moseley and Goode, 2005; Moseley et al., 2004). Therefore, two activators of *Ag*Bni1, *Ag*Cdc42 and *Ag*Bud6, are restricted to the cortex, while *Ag*Bni1 itself is also found in the center of the Spitzenkörper where no homolog of known *Ag*Bni1 activators was enriched. Interestingly, also in budding yeast, *Sc*Bni1 localizes to sites of polar growth, together with Rho-type GTP-binding proteins and *Sc*Bud6, and to sites in the cytoplasm. It was found that *Sc*Bni1 dynamically localizes to the bud tip, where it mediates formation of actin cables. At the same time, it is incorporated in actin filaments and redispersed by the continuous retrograde actin flow, leading to the observed cytoplasmatic *Sc*Bni1-speckles (Buttery et al., 2007). If we assume a similar mechanism in *A. gossypii*, simple clustering of cable-associated, inactive *Ag*Bni1 may lead to the observed *Ag*Bni1 concentration in the Spitzenkörper and, at the same time, may focus actin cables at this site.

As in *A. gossypii*, the *A. nidulans* formin SepA localizes to a defined spot in the Spitzenkörper (Harris et al., 2005). Furthermore, distinct core regions are observed in the Spitzenkörper of other fungi (Grove and Bracker, 1970; Lopez-Franco and Bracker Charles, 1996). These findings suggest that the Spitzenkörper is not only a plain vesicle accumulation but shows some degree of organization. Interestingly, the concept of a polarized vesicle-based structure that is involved in actin organization seems to be conserved even beyond fungi. In the green algae *Chara globularis*, actin filaments emanate from a Spitzenkörper that is located in the tips of rhizoids, which are tubular gravity-sensing cells (Braun et al., 1999; Braun et al., 2004). Spitzenkörper are thus present in a wide variety of organisms: in *A. gossypii*, which is closely related to budding yeast and which does not rely on microtubules for tip growth; in the hyphal form of the dimorphic fungus *C. albicans* (Crampin et al., 2005); in many filamentous ascomycete and basidiomycetes; and even in filamentous plant cells. This argues that, although it may have different evolutionary origins in these organisms, the Spitzenkörper constitutes a very successful adaptation to the demands of fast filamentous growth of walled cells.

Materials and Methods

A. gossypii growth conditions

A. gossypii media, culturing and transformation protocols are described by Ayad-Durieux et al. and by Wendland et al. (Ayad-Durieux et al., 2000; Wendland et al., 2000).

Cytoskeleton disruption, staining and immunofluorescence

The actin cytoskeleton was stained (see Knechtle et al., 2003). Anti-tubulin immunofluorescence was carried out as described previously (see Gladfelter et al., 2006). A rat anti-tubulin antibody (YOL34; Serotec, Kidlington, UK) was used at a dilution of 1:50, AlexaFluor568 goat anti-rat (Invitrogen, Carlsbad CA, USA) at a dilution of 1:200. Nocodazole (Sigma-Aldrich, St Louis, MO), 15 μg/ml for liquid and 30 μg/ml for solid medium, was used to disrupt microtubules. The actin cytoskeleton was disrupted with final concentrations of 200 μM latrunculin A in liquid and 400 μM on solid medium. Control treatments were performed with DMSO.

DNA manipulation, plasmids and oligonucleotides

All DNA manipulations were carried out according to Sambrook (Sambrook, 2001). The *E. coli* strain DH5alphaF' (Hanahan, 1983) was used as a host. PCR was performed using Taq DNA polymerase, the Expand High Fidelity PCR system or the Expand Long Template PCR system (Roche Diagnostics, Mannheim, Germany). Oligonucleotides (see Table S1 in the supplementary material) were synthesized either by MWG (Ebersberg, Germany) or Microsynth (Balgach, Switzerland). Plasmids were constructed as described in Table S2 in the supplementary material.

A. gossypii strain construction

A. gossypii strains are listed in Table S3 in the supplementary material. *Agleu2ΔAgthr4Δ* (Altmann-Johl and Philippsen, 1996) was used for all transformations unless indicated otherwise and is referred to as *wt*. Homologous integration of the transforming DNA was verified by analytical PCR in the primary transformants (heterokaryotic, nuclei with different genetic configurations share a common cytoplasm) and in clonally purified strains (homokaryotic, nuclei are genetically identical).

Gene deletions

Genes were deleted using the PCR-based one-step gene targeting approach with heterologous markers (see Wendland et al., 2000) or using an indirect plasmid-based approach. The name of the respective oligonucleotides, PCR templates and plasmids used to produce the deletion cassettes can be found in the *A. gossypii* strain table

(see Table S3 in the supplementary material). The *GEN3* cassette (Wendland et al., 2000) mediates resistance against G418, and the *NAT1* cassette (D. Hoepfner, personal communication) mediates resistance against ClonNat (Werner Bioagents, Jena, Germany).

GFP fusions

Fusions to GFP or YFP were accomplished by co-transformation of a PCR-generated cassette with an ARS-CEN vector containing the *A. gossypii* gene into the yeast strain *DHD5* (Arvanitidis and Heinisch, 1994). The resulting plasmids were digested with the restriction enzymes indicated in Table S3 (see supplementary material) and used for transformation of *A. gossypii*. GFP-fusion constructs were integrated into the genome replacing the wild-type genes. Expression was driven by the native promoter except for *K47* and *K52*, where *GFP-AgBNI1* and *GFP-AgBUD6* are under control of the *S. cerevisiae HIS3* promoter. Western blot analysis showed that the *ScHIS3* driven expression of *GFP-AgBNI*1 (*K47*) resulted in five to ten times increased proteins levels (not shown). The presented results were obtained with *K47*, the localization patterns and speed dependences observed for the *AgBNI1* promoter driven *GFP-AgBNI1* expression (*K46*) were similar but signal strength, and thus image quality, was lower.

Agcdc42Δ GFP-CDC42 (pK49): a selection-based process for generation of GFP-fusions constructs

A GFP-*Ag*Cdc42 fusion constructed analogous to GFP-*Ag*Rho1a (Kohli et al., 2008) was not functional. Therefore, a random linker library was inserted between *GFP* and *AgCDC42* on pK12 by homologous recombination in the yeast strain *DLY3067* (Moskow et al., 2000). The random linkers, which consisted of nine SNY-repeats (S: G or C, N: G,A,T or C, Y: T or C) and flanking regions were created in a PCR-based fill-in reaction from the oligonucleotides 05.301 and 05.302. Functional *GFP-AgCDC42* fusion constructs were selected on glucose that shuts down production of *Sc*Cdc42 in *DLY3067*. A heterokaryotic *Agcdc42Δ* strain was transformed with the rescued pK49 library. Plasmids containing an ARS sequence from yeast can replicate in *A. gossypii* and are not integrated into the genome (Wright and Philippsen, 1991). Clonal purification resulted in *A. gossypii* strains that were homokaryotic for the genomic *AgCDC42* deletion expressing GFP-*Ag*Cdc42 from a plasmid, which was verified by analytical PCR. Radial growth speed was estimated to select for fusion constructs that displayed maximal radial growth speeds. The random linker of the strain used for this study was coding for the peptide APPRRLVHP. Similar results were obtained with strains that differed in the random linker sequence (not shown).

Light microscopy, sample preparation and image processing

The microscope set up is described by Knechtle et al. (Knechtle et al., 2003); the camera was a CoolSNAP HQ camera (Photometrics, Tucson AZ, USA). A 75 W XBO short arc lamp (Osram, Augsburg, Germany) or a Polychrome V monochromator (Till Photonics, Gräfelfing, Germany) served as illumination sources. Mycelium from the borders of 3-day-old *A. gossypii* colonies was inoculated on glass slides with a cavity (Roth, Reinach, Switzerland) filled with half-strength AFM agarose. 4 µl of 11 µM FM4-64 in AFM was applied directly on the sample if not mentioned otherwise. FM4-64-stained Spitzenkörper were observed after 10 minutes of incubation, stained samples were discarded 1 hour after dye addition. DIC images were processed using the 'Unsharp Mask' feature from MetaMorph 6.2r6 (Molecular Devices, Downingtown, PA). Stacks with a *z*-distance between 0.3 and 0.8 µm were acquired and processed either with the 'Remove Haze' function or the 'Nearest Neighbour' tool of MetaMorph. Overlays were carried out with the 'Overlay Images' function of MetaMorph. Stacks that were used for blind deconvolution with AutoDeblur 7 (MediaCybernetics, Silver Spring MD, USA) contained at least 32 image planes with a *z*-distance of maximally 0.3 µm. The fluorescence images shown are maximum or sum projections of two to four central planes of processed image stacks.

Measurements

Measurements were done with MetaMorph 6.2r6 on the plane of an image stack that was closest to the hyphal centre. Growth speed was measured by acquisition of a DIC image followed by a time interval of 150 seconds and a DIC image stack. The cortical zone where *Ag*Exo70-GFP was enriched was approximated as a spherical cap. For measurements, the lower scaling value was set to the value of the maximal fluorescence in a 5 µm circle whose centre was located 10 µm behind the tip. Standard errors of the mean (s.e.m.) are given throughout this study.

Transmission electron microscopy (TEM)

Sample preparation for TEM was performed according to McDaniel and Roberson (McDaniel and Roberson, 2000). Mycelia were inoculated on thin dialysis membranes on AFM agar overnight at room temperature. Membranes with *A. gossypii* colonies were plunge-frozen in a liquid propane-ethene mixture. Freeze-substitution took place in 1% glutaraldehyde and 1% tannic acid (w/v) in anhydrous acetone at –80°C for 72 hours. After washing in acetone, the samples were warmed up stepwise in a 1% OsO_4 solution in acetone and flat-embedded in Spurr's resin (Spurr, 1969). Selected hyphae were sectioned and post-stained in 2% uranyl-acetate in 50% ethanol and in Reynolds' lead citrate (Reynolds, 1963), sections were examined using a Philips CM12S TEM (Philips Electronic Instruments, Mahwah, NJ).

M.K. thanks R.W.R. for generous support during his 4 months electron microscopy training. We are very grateful to Daniele Cavicchioli and Philipp Knechtle for providing the *Ag*Bem1-GFP strain prior to publication, to Andreas Kaufmann for sharing new *A. gossypii* gene targeting cassettes, to Dominc Hoepfner for the *NAT1* cassette, to Sylvia Voegeli for bioinformatics support and to David Drubin for yeast strains. We thank Sandrine Grava, Andreas Kaufmann, Hans-Peter Helfer and Katrin Hungerbühler for helpful comments on the manuscript. We also acknowledge the help of Sandra Gass, Stéphanie Hauselmann and Déborah Ley in strain constructions. The work was supported by a training grant form the Swiss Federal Department of Home Affairs (ELTEM-Biotechnology) and by research grants from the University of Basel.

References

Adamo, J. E., Rossi, G. and Brennwald, P. (1999). The Rho GTPase Rho3 has a direct role in exocytosis that is distinct from its role in actin polarity. *Mol. Biol. Cell* **10**, 4121-4133.

Akashi, T., Kanbe, T. and Tanaka, K. (1994). The role of the cytoskeleton in the polarized growth of the germ tube in Candida albicans. *Microbiology* **140**, 271-280.

Altmann-Johl, R. and Philippsen, P. (1996). AgTHR4, a new selection marker for transformation of the filamentous fungus Ashbya gossypii, maps in a four-gene cluster that is conserved between A. gossypii and Saccharomyces cerevisiae. *Mol. Gen. Genet.* **250**, 69-80.

Arvanitidis, A. and Heinisch, J. J. (1994). Studies on the function of yeast phosphofructokinase subunits by *in vitro* mutagenesis. *J. Biol. Chem.* **269**, 8911-8918.

Ashby, S. F. and Nowell, W. (1926). The fungi of stigmatomycosis. *Annals of Botany* **40**, 69-84.

Ayad-Durieux, Y., Knechtle, P., Goff, S., Dietrich, F. and Philippsen, P. (2000). A PAK-like protein kinase is required for maturation of young hyphae and septation in the filamentous ascomycete Ashbya gossypii. *J. Cell Sci.* **113**, 4563-4575.

Ayscough, K. R., Stryker, J., Pokala, N., Sanders, M., Crews, P. and Drubin, D. G. (1997). High rates of actin filament turnover in budding yeast and roles for actin in establishment and maintenance of cell polarity revealed using the actin inhibitor latrunculin-A. *J. Cell Biol.* **137**, 399-416.

Bartnicki-Garcia, S. and Lippman, E. (1969). Fungal morphogenesis: cell wall construction in Mucor rouxii. *Science* **165**, 302-304.

Bartnicki-Garcia, S., Hergert, F. and Gierz, G. (1989). Computer simulation of fungal morphogenesis and the mathematical basis for hyphal (tip) growth. *Protoplasma* **153**, 46-57.

Bourett, T. M. and Howard, R. J. (1991). Ultrastructural immunolocalization of actin in a fungus. *Protoplasma* **163**, 199-202.

Boyd, C., Hughes, T., Pypaert, M. and Novick, P. (2004). Vesicles carry most exocyst subunits to exocytic sites marked by the remaining two subunits, Sec3p and Exo70p. *J. Cell Biol.* **167**, 889-901.

Braun, M., Buchen, B. and Sievers, A. (1999). Ultrastructure and cytoskeleton of Chara rhizoids in microgravity. *Adv. Space Res.* **24**, 707-711.

Braun, M., Hauslage, J., Czogalla, A. and Limbach, C. (2004). Tip-localized actin polymerization and remodeling, reflected by the localization of ADF, profilin and villin, are fundamental for gravity-sensing and polar growth in characean rhizoids. *Planta* **219**, 379-388.

Buttery, S. M., Yoshida, S. and Pellman, D. (2007). Yeast formins Bni1 and Bnr1 utilize different modes of cortical interaction during the assembly of actin cables. *Mol. Biol. Cell* **18**, 1826-1838.

Collinge, A. J. and Trinci, A. P. (1974). Hyphal tips of wild-type and spreading colonial mutants of Neurospora crassa. *Arch. Microbiol.* **99**, 353-368.

Crampin, H., Finley, K., Gerami-Nejad, M., Court, H., Gale, C., Berman, J. and Sudbery, P. (2005). Candida albicans hyphae have a Spitzenkorper that is distinct from the polarisome found in yeast and pseudohyphae. *J. Cell Sci.* **118**, 2935-2947.

Dietrich, F. S., Voegeli, S., Brachat, S., Lerch, A., Gates, K., Steiner, S., Mohr, C., Pohlmann, R., Luedi, P., Choi, S. et al. (2004). The Ashbya gossypii genome as a tool for mapping the ancient Saccharomyces cerevisiae genome. *Science* **304**, 304-307.

Evangelista, M., Blundell, K., Longtine, M. S., Chow, C. J., Adames, N., Pringle, J. R., Peter, M. and Boone, C. (1997). Bni1p, a yeast formin linking cdc42p and the actin cytoskeleton during polarized morphogenesis. *Science* **276**, 118-122.

Finger, F. P., Hughes, T. E. and Novick, P. (1998). Sec3p is a spatial landmark for polarized secretion in budding yeast. *Cell* **92**, 559-571.

Fischer-Parton, S., Parton, R. M., Hickey, P. C., Dijksterhuis, J., Atkinson, H. A. and Read, N. D. (2000). Confocal microscopy of FM4-64 as a tool for analysing endocytosis and vesicle trafficking in living fungal hyphae. *J. Microsc.* **198**, 246-259.

France, Y. E., Boyd, C., Coleman, J. and Novick, P. J. (2006). The polarity-establishment component Bem1p interacts with the exocyst complex through the Sec15p subunit. *J. Cell Sci.* **119**, 876-888.

Fuchs, U., Manns, I. and Steinberg, G. (2005). Microtubules are dispensable for the initial pathogenic development but required for long-distance hyphal growth in the corn smut fungus Ustilago maydis. *Mol. Biol. Cell* **16**, 2746-2758.

Fujiwara, T., Tanaka, K., Mino, A., Kikyo, M., Takahashi, K., Shimizu, K. and Takai, Y. (1998). Rho1p-Bni1p-Spa2p interactions: implication in localization of Bni1p at the bud site and regulation of the actin cytoskeleton in Saccharomyces cerevisiae. *Mol. Biol. Cell* **9**, 1221-1233.

Gierz, G. and Bartnicki-Garcia, S. (2001). A three-dimensional model of fungal morphogenesis based on the vesicle supply center concept. *J. Theor. Biol.* **208**, 151-164.
Gladfelter, A. S., Hungerbuehler, A. K. and Philippsen, P. (2006). Asynchronous nuclear division cycles in multinucleated cells. *J. Cell Biol.* **172**, 347-362.
Grove, S. N. and Bracker, C. E. (1970). Protoplasmic organization of hyphal tips among fungi: vesicles and Spitzenkorper. *J. Bacteriol.* **104**, 989-1009.
Guo, W., Roth, D., Walch-Solimena, C. and Novick, P. (1999). The exocyst is an effector for Sec4p, targeting secretory vesicles to sites of exocytosis. *EMBO J.* **18**, 1071-1080.
Guo, W., Tamanoi, F. and Novick, P. (2001). Spatial regulation of the exocyst complex by Rho1 GTPase. *Nat. Cell Biol.* **3**, 353-360.
Hanahan, D. (1983). Studies on transformation of Escherichia coli with plasmids. *J. Mol. Biol.* **166**, 557-580.
Harris, S. D., Read, N. D., Roberson, R. W., Shaw, B., Seiler, S., Plamann, M. and Momany, M. (2005). Polarisome meets spitzenkorper: microscopy, genetics, and genomics converge. *Eukaryot. Cell* **4**, 225-229.
Holly, S. P. and Blumer, K. J. (1999). PAK-family kinases regulate cell and actin polarization throughout the cell cycle of Saccharomyces cerevisiae. *J. Cell Biol.* **147**, 845-856.
Horio, T. and Oakley, B. R. (2005). The role of microtubules in rapid hyphal tip growth of Aspergillus nidulans. *Mol. Biol. Cell* **16**, 918-926.
Huckaba, T. M., Gay, A. C., Pantalena, L. F., Yang, H. C. and Pon, L. A. (2004). Live cell imaging of the assembly, disassembly, and actin cable-dependent movement of endosomes and actin patches in the budding yeast, Saccharomyces cerevisiae. *J. Cell Biol.* **167**, 519-530.
Jin, H. and Amberg, D. C. (2000). The secretory pathway mediates localization of the cell polarity regulator Aip3p/Bud6p. *Mol. Biol. Cell* **11**, 647-661.
Kaksonen, M., Sun, Y. and Drubin, D. G. (2003). A pathway for association of receptors, adaptors, and actin during endocytic internalization. *Cell* **115**, 475-487.
Karpova, T. S., Reck-Peterson, S. L., Elkind, N. B., Mooseker, M. S., Novick, P. J. and Cooper, J. A. (2000). Role of actin and Myo2p in polarized secretion and growth of Saccharomyces cerevisiae. *Mol. Biol. Cell* **11**, 1727-1737.
Knechtle, P., Dietrich, F. and Philippsen, P. (2003). Maximal polar growth potential depends on the polarisome component AgSpa2 in the filamentous fungus Ashbya gossypii. *Mol. Biol. Cell* **14**, 4140-4154.
Knechtle, P., Wendland, J. and Philippsen, P. (2006). The SH3/PH domain protein AgBoi1/2 collaborates with the Rho-type GTPase AgRho3 to prevent nonpolar growth at hyphal tips of Ashbya gossypii. *Eukaryot. Cell* **5**, 1635-1647.
Kohli, M., Buck, S. and Schmitz, H. P. (2008). The function of two closely related Rho proteins is determined by an atypical switch I region. *J. Cell Sci.* **121**, 1065-1075.
Li, C. R., Lee, R. T., Wang, Y. M., Zheng, X. D. and Wang, Y. (2007). Candida albicans hyphal morphogenesis occurs in Sec3p-independent and Sec3p-dependent phases separated by septin ring formation. *J. Cell Sci.* **120**, 1898-1907.
Lopez-Franco, R. and Bracker, C. E. (1996). Diversity and dynamics of the Spitzenkörper in growing hyphal tips of higher fungi. *Protoplasma* **195**, 90-111.
McDaniel, D. P. and Roberson, R. W. (2000). Microtubules Are required for motility and positioning of vesicles and mitochondria in hyphal tip cells of Allomyces macrogynus. *Fungal Genet. Biol.* **31**, 233-244.
Moseley, J. B. and Goode, B. L. (2005). Differential activities and regulation of Saccharomyces cerevisiae formin proteins Bni1 and Bnr1 by Bud6. *J. Biol. Chem.* **280**, 28023-28033.
Moseley, J. B., Sagot, I., Manning, A. L., Xu, Y., Eck, M. J., Pellman, D. and Goode, B. L. (2004). A conserved mechanism for Bni1- and mDia1-induced actin assembly and dual regulation of Bni1 by Bud6 and profilin. *Mol. Biol. Cell* **15**, 896-907.
Moskow, J. J., Gladfelter, A. S., Lamson, R. E., Pryciak, P. M. and Lew, D. J. (2000). Role of Cdc42p in pheromone-stimulated signal transduction in Saccharomyces cerevisiae. *Mol. Cell. Biol.* **20**, 7559-7571.
Ozaki-Kuroda, K., Yamamoto, Y., Nohara, H., Kinoshita, M., Fujiwara, T., Irie, K. and Takai, Y. (2001). Dynamic localization and function of Bni1p at the sites of directed growth in Saccharomyces cerevisiae. *Mol. Cell. Biol.* **21**, 827-839.
Park, H. O. and Bi, E. (2007). Central roles of small GTPases in the development of cell polarity in yeast and beyond. *Microbiol. Mol. Biol. Rev.* **71**, 48-96.
Reynolds, E. S. (1963). The use of lead citrate at high pH as an electron-opaque stain in electron microscopy. *J. Cell Biol.* **17**, 208-212.
Riquelme, M., Bartnicki-Garcia, S., Gonzalez-Prieto, J. M., Sanchez-Leon, E., Verdin-Ramos, J. A., Beltran-Aguilar, A. and Freitag, M. (2007). Spitzenkorper localization and intracellular traffic of green fluorescent protein-labeled CHS-3 and CHS-6 chitin synthases in living hyphae of Neurospora crassa. *Eukaryot. Cell* **6**, 1853-1864.
Sambrook, J. a. D. R. (2001). *Molecular Cloning: A Laboratory Manual*. Cold Spring Harbor: Cold Spring Harbor Laboratory Press.
Schmitz, H. P., Kaufmann, A., Kohli, M., Laissue, P. P. and Philippsen, P. (2006). From function to shape: a novel role of a formin in morphogenesis of the fungus ashbya gossypii. *Mol. Biol. Cell* **17**, 130-145.
Sharpless, K. E. and Harris, S. D. (2002). Functional characterization and localization of the Aspergillus nidulans formin SEPA. *Mol. Biol. Cell* **13**, 469-479.
Sheu, Y. J., Santos, B., Fortin, N., Costigan, C. and Snyder, M. (1998). Spa2p interacts with cell polarity proteins and signaling components involved in yeast cell morphogenesis. *Mol. Cell. Biol.* **18**, 4053-4069.
Shih, J. L., Reck-Peterson, S. L., Newitt, R., Mooseker, M. S., Aebersold, R. and Herskowitz, I. (2005). Cell polarity protein Spa2P associates with proteins involved in actin function in Saccharomyces cerevisiae. *Mol. Biol. Cell* **16**, 4595-4608.
Snyder, M. (1989). The SPA2 protein of yeast localizes to sites of cell growth. *J. Cell Biol.* **108**, 1419-1429.
Srijayanthi, S., Vargas, M. and Roberson, R. W. (1996). Functional, organizational, and biochemical analysis of actin in the hyphal tip cells of Allomyces macrogynus. *Mycologia* **88**, 57-70.
Steinberg, G. (2007). Hyphal growth: a tale of motors, lipids, and the Spitzenkorper. *Eukaryot. Cell* **6**, 351-360.
Taheri-Talesh, N., Horio, T., Araujo-Bazan, L., Dou, X., Espeso, E. A., Penalva, M. A., Osmani, S. A. and Oakley, B. R. (2008). The tip growth apparatus of aspergillus nidulans. *Mol. Biol. Cell* **19**, 1439-1449.
TerBush, D. R., Maurice, T., Roth, D. and Novick, P. (1996). The Exocyst is a multiprotein complex required for exocytosis in Saccharomyces cerevisiae. *EMBO J.* **15**, 6483-6494.
Torralba, S., Raudaskoski, M., Pedregosa, A. M. and Laborda, F. (1998). Effect of cytochalasin A on apical growth, actin cytoskeleton organization and enzyme secretion in Aspergillus nidulans. *Microbiology* **144**, 45-53.
Valtz, N. and Herskowitz, I. (1996). Pea2 protein of yeast is localized to sites of polarized growth and is required for efficient mating and bipolar budding. *J. Cell Biol.* **135**, 725-739.
Virag, A. and Harris, S. D. (2006). Functional characterization of Aspergillus nidulans homologues of Saccharomyces cerevisiae Spa2 and Bud6. *Eukaryot. Cell* **5**, 881-895.
Wedlich-Soldner, R., Altschuler, S., Wu, L. and Li, R. (2003). Spontaneous cell polarization through actomyosin-based delivery of the Cdc42 GTPase. *Science* **299**, 1231-1235.
Wendland, J. and Philippsen, P. (2001). Cell polarity and hyphal morphogenesis are controlled by multiple rho-protein modules in the filamentous ascomycete Ashbya gossypii. *Genetics* **157**, 601-610.
Wendland, J., Ayad-Durieux, Y., Knechtle, P., Rebischung, C. and Philippsen, P. (2000). PCR-based gene targeting in the filamentous fungus Ashbya gossypii. *Gene* **242**, 381-391.
Wright, M. C. and Philippsen, P. (1991). Replicative transformation of the filamentous fungus Ashbya gossypii with plasmids containing Saccharomyces cerevisiae ARS elements. *Gene* **109**, 99-105.
Zajac, A., Sun, X., Zhang, J. and Guo, W. (2005). Cyclical regulation of the exocyst and cell polarity determinants for polarized cell growth. *Mol. Biol. Cell* **16**, 1500-1512.
Zhang, X., Bi, E., Novick, P., Du, L., Kozminski, K. G., Lipschutz, J. H. and Guo, W. (2001). Cdc42 interacts with the exocyst and regulates polarized secretion. *J. Biol. Chem.* **276**, 46745-46750.